Available online at http://www.journalcra.com

International Journal of Current Research
Vol. 5, Issue, 06, pp.1473-1483, June, 2013

INTERNATIONAL JOURNAL OF CURRENT RESEARCH

ISSN: 0975-833X

RESEARCH ARTICLE

A NON-NEWTONIAN HERSCHEL-BULKLEY MODEL FOR BLOOD FLOW THROUGH A CATHETERIZED TAPERED ARTERY

[1]Dr. Meena, K., [2]Gayathri, P. and [3]Dr. Subramanian, K. R.

[1] Vice-Chancellor, Bharathidasan University, Trichy, Tamil Nadu, India
[2]Research scholar, Department of Mathematics and Computer Applications, Shrimati Indira Gandhi College, Trichy
[3] Professor, Department of Computer Applications, Shrimati Indira Gandhi College, Trichy

ARTICLE INFO

Article History:
Received 16th March, 2013
Received in revised form
19th April, 2013
Accepted 23rd May, 2013
Published online 15th June, 2013

Key words:
Non- Newtonian fluid,
Tapered Artery,
Steady flow, Catheter.
AMS Subject Classification (1991):
760z05, 92c35

ABSTRACT

The steady flow of through a catheterized tapered artery with a stenosis is analyzed, assuming the blood as a non-Newtonian Herschel-Bulkley fluid. A system of non linear partial differential equations for blood flow of the artery was obtained. The governing equations are solved using calculus method. The width of the plug flow region increases with the increase of the yield stress, and the reverse behavior is noticed when the steady state pressure gradient increases when all the other parameters are kept fixed. It is observed that the velocity and flow rate decrease while the wall shear stress and resistance to flow increase when the yield stress or catheter radius ratio or angle of tapering increases while all the other parameters held fixed.

INTRODUCTION

The study of blood flow through an inserted catheter has been the subject of scientific research for a long time. Its plays an important role in the fundamental understanding, diagnosis and treatment of cardiovascular system. Like most of the problem of nature and life sciences. It is complex one due to the complicated structure of blood, the circulatory system and their constituent materials. The experimental studies and the theoretical treatment of blood flow phenomena are very useful for the diagnosis of a number of cardiovascular diseases and development of pathological patterns in human or animal physiology and for other clinical purposes and practical applications (Srivastava and Srivastava 1983). Blood is composed of fluid plasma and formed elements. The formed elements of blood are erythrocyte, leukocyte and platelets. The percentage volume of red cells is called the haematocrit and is approximately 40- 45 % (Oka, 1973) for an adult. Red cells may affect the viscosity of whole blood considered as homogenous fluid. In general, Blood is known to be an incompressible non-Newtonian Fluid. This property is mainly the result of cell concentration (Demiray 2003). However in the course of flow in arteries, the red blood cells in the vicinity of arterial wall move to the central region of the artery. So that the haematocrit ratio becomes quite low near the arterial wall, which results in lower viscosity in this region. A catheter is made of polyester based thermoplastic polyurethane, medical grade polyvinyl chloride etc. For the purpose of flexibility PVC materials containing added plasticizers are used in catheter which enables them to move through the branches or curved paths of the circulatory system. Transducers attached to catheters are of large usage in clinical works and the techniques are used for measuring blood pressure or other mechanical properties in arteries (Anderson *et al*., 1986). In all the investigation blood has treated as a Newtonian fluid. Recently, Sankar and Hemlatha (2006-2007) addressed the problem of pulsatile flow of Hershel-Bulkey fluid in catheterized arteries. Dash et.al. (1999) studied the changed flow pattern in narrow artery when a catheter is inserted into it and estimate the increase in friction in the artery due to catheterization using Casson fluid model for steady and pulsatile flow of blood.

Formulation of the Mathematical model

Consider an axially symmetric, laminar steady and fully developed flow of blood assumed to be incompressible in the axial direction $(\bar{z})$ through a circular rigid tapered artery in which an axially symmetric mild stenosis. A catheter is introduced coaxially, where the artery is modelled as a constricted tapered circular tube of radius $\overline{R}$ and the catheter radius is taken to be K $\overline{R}$ (0<K<1). It is assumed that the blood is modelled as a single fluid model with as a non-Newtonian Herschel-Bulkley fluid. The tapered vessel segment having an axially symmetric stenosis with catheter is mathematically modelled as a rigid tube with a circular section and a catheter is coaxial to it. We have used the cylindrical polar co-ordinates $(\bar{r}, \bar{\phi}, \bar{z})$ where $\bar{r}$ and $\bar{z}$ denote the radial and axial co-ordinates and $\bar{\phi}$ is the azimuthal angle. The radial velocity is negligibly small in magnitude and may be neglected for low Reynolds number flow and the pressure gradient is a function of $\bar{z}$ alone. The study have been considered on catheterized tapered artery with mild stenosis the proposed momentum equation of the flow is as follows

Corresponding author: gay_sundar@yahoo.co.in

$$\frac{d\bar{p}}{d\bar{z}} = -\frac{1}{\bar{r}}\frac{d}{d\bar{r}}(\bar{r}\bar{\tau}_H) \text{ in } K\bar{R} \le \bar{r} \le \bar{R}(\bar{z}) \quad (1)$$

where $\bar{p}$ denotes the pressure, $\bar{\tau}_H$ denote the shear stress of the Herschel – Bulkley fluid and $\bar{R}$ is the radius of the of the normal artery respectively. $\bar{R}\left(\bar{z}\right)$ is the radius of the tapered artery in the stenosed region.

The proposed constitutive equations of the fluid motion in the core region (Herschel – Bulkley fluid) are given by

$$\bar{\mu}_H \left|\frac{\partial \bar{u}_H}{\partial \bar{r}}\right| = \left(\left|\bar{\tau}_H\right| - \bar{\tau}_y\right)^n$$

$$\text{if } \left|\bar{\tau}_H\right| \ge \bar{\tau}_y \text{ and } K\bar{R} \le \bar{r} \le \lambda_1\bar{R} \text{ and } \lambda_2\bar{R}_0 \le \bar{r} \le \bar{R}_0(\bar{z}) \quad (2)$$

$$\text{and } \frac{\partial \bar{u}_H}{\partial \bar{r}} = 0 \text{ if } \left|\bar{\tau}_H\right| \le \bar{\tau}_y \text{ and } \lambda_1\bar{R} \le \bar{r} \le \lambda_2\bar{R} \quad (3)$$

where $\overline{u_H}$ is the axial component of fluid's velocity, $\overline{\mu_H}$ is the viscosity of the Herschel – Bulkley fluid. $\overline{\tau_y}$ is the yield stress, λ_1 and λ_2 are the yield planes bounding of the plug flow region, n is the power law index. From equation (4) it is clear that the velocity gradient vanishes in the region where the shear stress is less than the yield stress which implies a plug flow whenever $\overline{\tau_H} \le \overline{\tau_y}$. However, the fluid behavior is indicated whenever $\overline{\tau_H} \ge \overline{\tau_y}$. The equivalent form of the constitutive equations form (2) - (3) when the shear stress and strain rate have opposite signs and when $\left|\overline{\tau_H}\right| \ge \bar{\tau}_y$ can be written as

$$\bar{\mu}_H \frac{\partial \bar{u}_H}{\partial \bar{r}} = \left(\left|\bar{\tau}_H\right| - \bar{\tau}_y\right)^n \text{ for } \frac{\partial \bar{u}_H}{\partial \bar{r}} > 0 \text{ and } \bar{\tau}_H < 0 \text{ and K}\,\bar{R} \le \bar{r} \le \lambda_1\bar{R} \quad (4)$$

$$\bar{\mu}_H \frac{\partial \bar{u}_H}{\partial \bar{r}} = \left(\left|\bar{\tau}_H\right| - \bar{\tau}_y\right)^n \text{ for } \frac{\partial \bar{u}_H}{\partial \bar{r}} < 0 \text{ and } \bar{\tau}_H > 0 \text{ and } \lambda_2\bar{R} \le \bar{r} \le \bar{R}(\bar{z}) \quad (5)$$

$$\frac{\partial \bar{u}_H}{\partial \bar{r}} = 0 \text{ if } \left|\bar{\tau}_H\right| \le \bar{\tau}_y \text{ and } \lambda_1\bar{R} \le \bar{r} \le \lambda_2\bar{R} \quad (6)$$

The equations in (4) and (5) constitute a non-linear coupled implicit system of differential equations governing the time-independent one dimensional shear flow of a Herschel – Bulkley fluid. These are to be solved subject to appropriate boundary conditions. It is assumed that the time elapsed from the start of motion is large enough to ignore the initial and transient effects. Then the boundary conditions are appropriate for the problem under study is the no slip condition at both the walls, that is,

$$\overline{u_H} = 0 \text{ at } \bar{r} = K\bar{R} \text{ and}$$

$$\overline{u_H} = 0 \text{ at } \bar{r} = \bar{R}(\bar{z}) \quad (7)$$

The geometry of the constricted tapered stenosed artery is mathematically modelled as

$$\bar{R}(\bar{z}) = \begin{cases} \bar{R} - m(\bar{z} + \bar{d}) - \dfrac{\bar{\delta}_H \cos\alpha}{2}\left(1 + \cos\dfrac{\pi\bar{z}}{\bar{z}_0}\right), \left|\bar{z}\right| \le \bar{z}_0 \\ \bar{R} - m(\bar{z} + \bar{d}), \left|\bar{z}\right| > \bar{z}_0 \end{cases} \quad (8)$$

where $\bar{R}(\bar{z})$ is the radius of the tapered artery in stenosed region, α is the angle of tapering, $\overline{\delta_H}$ is the maximum projection of the stenosis, $\overline{\delta_H}Cos\alpha$ is the length of the stenosis at a length $\bar{d}$ for the tapered artery in the stenotic region, $2\bar{z}_0$ is the length of the stenosis and m(= tan α) represents the slope of the tapered vessel, $\bar{R}$ is the constant radius of the normal artery.

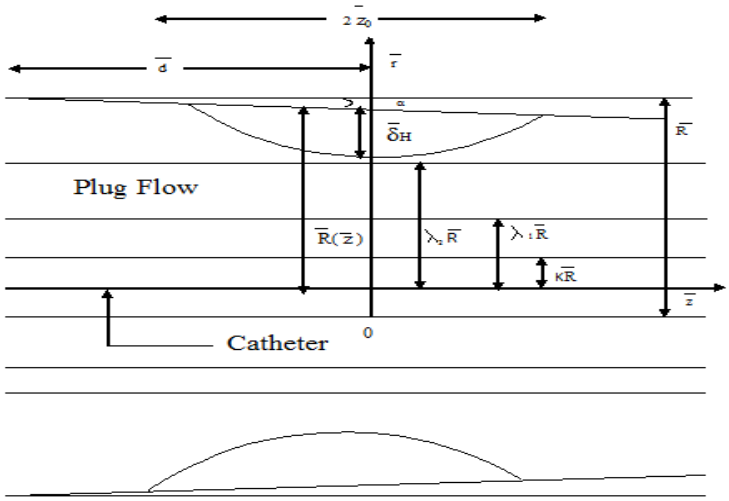

Geometry of Single layered catheterized tapered artery with stenosis

Let us introduce the following non-dimensional variables,

$$u_H = \frac{\bar{u}_H}{\frac{\bar{p}_0 \bar{R}^2}{2\bar{\mu}_0}}, r = \frac{\bar{r}}{\bar{R}}, R(z) = \frac{\bar{R}(\bar{z})}{\bar{R}}, z = \frac{\bar{z}}{\bar{R}}, \tau_H = \frac{\bar{\tau}_H}{\frac{\bar{p}_0 \bar{R}}{2}},$$

$$\tau_y = \frac{\bar{\tau}_y}{\frac{\bar{p}_0 \bar{R}}{2}}, d = \frac{\bar{d}}{\bar{R}}, \delta_H = \frac{\bar{\delta}_H}{\bar{R}}, z_0 = \frac{\bar{z}_0}{\bar{R}}, KR = \frac{K\bar{R}}{\bar{R}} \tag{9}$$

where $\bar{\mu}_0 = \bar{\mu}_H \left(2/\bar{p}_0 \bar{R} \right)^{n-1}$ and $\bar{p}_0$ is the absolute magnitude of the typical pressure gradient, τ_y is the non-dimensional yield stress. Since the flow is assumed as steady, the pressure gradient can be written as

$$\frac{d\bar{p}}{d\bar{z}} = -\bar{p}_0 P \tag{10}$$

where P is the non-dimensional steady state pressure gradient.

The geometry of the stenosis (in the dimensionless form) for the constricted tapered artery is mathematically modelled as

$$R(z) = \begin{cases} 1 - m(z+d) - \frac{\delta_H \cos\alpha}{2}\left(1 + \cos\frac{\pi z}{z_0}\right), |z| \le z_0 \\ 1 - m(z+d), |z| > z_0 \end{cases} \tag{11}$$

Using equations (9) and (10), the momentum equation in (1) is reduced to

$$2P = \frac{1}{r}\frac{d}{dr}\left(r\tau_H\right) \text{ in } K \le r \le R(z) \tag{12}$$

Similarly, using equations (9) and (10), the constitutive equations (4) - (6) are simplified, respectively to

$$\frac{du_H}{dr} = |\tau_H|^n \left(1 - \frac{n\tau_y}{|\tau_H|}\right) \text{for } \frac{du_H}{dr} > 0 \text{ , } \tau_H < 0 \text{ and } K \le r \le \lambda_1 \tag{13}$$

$$\frac{du_H}{dr} = \left|\tau_H\right|^n \left(1 - \frac{n\tau_y}{\left|\tau_H\right|}\right) \text{ for } \frac{du_H}{dr} < 0 \ , \quad \tau_H > 0 \text{ and } \lambda_2 \le r \le R(z) \tag{14}$$

$$\frac{du_H}{dr} = 0 \text{ if } \tau_H \le \tau_y \text{ and } \lambda_1 \le r \le \lambda_2 \tag{15}$$

The boundary conditions in the non-dimensional form are (no-slip)

$$u_H = 0 \text{ at } r = K \text{ and}$$
$$u_H = 0 \text{ at } r = R(z) \tag{16}$$

Integrating equation (13), we get

$$\tau_H = \Pr + \frac{c_1}{r} \tag{17}$$

where c_1 is the constant of integration.

From equations (13) to (15), it is clear that the flow in $K \le r \le R(z)$ is a three region one, in which the core region has a flat velocity profile and hence forms the plug flow region.In this plug flow region, where the shear stress does not exceed the yield stress, the fluid itself does not flow but is merely carried along by the fluid in the two adjacent viscous flow regions. For mathematical representation, the plug flow region can be defined as $\lambda_1 \le r \le \lambda_2$, where $K \le \lambda_1$ and $\lambda_2 \le R(z)$.

Here, λ_1 and λ_2 are unknown constants to be determined.
From the continuity of the shear stress along the boundary of the plug flow region,

$$-\tau_H = \tau_y \text{ for } r = \lambda_1 \text{ and}$$
$$\tau_H = \tau_y \text{ for } r = \lambda_2 \tag{18}$$
$$\therefore -\tau_H \,|_{r=\lambda_1} = \tau_y = \tau_H \,|_{r=\lambda_2} \tag{19}$$

By substituting equation (17) in equation (19), we get

$$-\mathrm{P}\left[\lambda_1 + \lambda_2\right] = c_1 \left[\frac{\lambda_1 + \lambda_2}{\lambda_1 \lambda_2}\right]$$
$$c_1 = -\mathrm{P}\lambda_1\lambda_2 \text{ and } c_1 = -\mathrm{P}\lambda^2 \tag{20}$$

where $\lambda^2 = \lambda_1\lambda_2$ (21)

By substituting equation (21) in equation (18), the shear stress of the Herschel-Bulkley fluid is given by

$$\tau_H = \Pr - \frac{P\lambda^2}{r}$$
$$\Rightarrow \tau_H = \frac{\mathrm{P}}{\mathrm{r}}\left[\mathrm{r}^2 - \lambda^2\right] \tag{22}$$

Using equation (22) in (19),

$$-\left[\frac{P}{r}\left(\mathrm{r}^2 - \lambda^2\right)\right]\Big|_{r=\lambda_1} = \tau_y$$
$$\Rightarrow \lambda_2 - \lambda_1 = \frac{\tau_y}{P} = \beta \tag{23}$$

where β is the width of the plug core region.

Let us consider the fluid velocity as $u_H^*, u_H^{**}, u_H^{***}$ for the regions corresponding to $K \le r \le \lambda_1$, $\lambda_1 \le r \le \lambda_2$ and $\lambda_2 \le r \le R(z)$ respectively. The expressions for the velocity in the three regions can be obtained from the (13) to (15),

$$\frac{du_H}{dr} = |\tau_H|^n \left(1 - \frac{n\tau_y}{|\tau_H|}\right)$$

$$\Rightarrow \frac{du_H}{dr} = |\tau_H|^n - n\tau_y |\tau_H|^{n-1} \tag{24}$$

Using $|\tau_H| = -\tau_H$ at $r = \lambda_1$ and using equations (20) and (23) in equation (24),

$$\frac{du_H^*}{dr} = |-\tau_H|^n - n\tau_y |-\tau_H|^{n-1}$$

$$\Rightarrow \frac{du_H^*}{dr} = \left[\frac{P}{n}\left(\lambda^2 - r^2\right)\right]^n - nP\beta\left[\frac{P}{r}\left(\lambda^2 - r^2\right)\right]^{n-1}$$

$$\frac{du_H^*}{dr} = P^n\left[\left(\frac{\lambda^2 - r^2}{r}\right)^n - n\beta\left(\frac{\lambda^2 - r^2}{r}\right)^{n-1}\right] \tag{25}$$

Integrating equation (25) from K to r with the help of the boundary conditions in equation (16), we get the initial approximation to the velocity u_H^* in the region $K \le r \le \lambda_1$ as

$$u_H^* = P^n\left[\int_K^r \left(\frac{\lambda^2 - r^2}{r}\right)^n dr - n\beta\int_K^r \left(\frac{\lambda^2 - r^2}{r}\right)^{n-1} dr\right] \tag{26}$$

For $\lambda_1 \le r \le \lambda_2$, $u_H^{**} = u_p(say)$

where u_p is a constant and u_p denotes the plug flow velocity.

The initial approximation to the plug flow velocity u_p in the region $\lambda_1 \le r \le \lambda_2$ can be obtained using the condition $u_p = u_H^*$ at $r = \lambda_1$ and is given by

$$u_p = P^n\left[\int_K^{\lambda_1} \left(\frac{\lambda^2 - r^2}{r}\right)^n dr - n\beta\int_K^{\lambda_1} \left(\frac{\lambda^2 - r^2}{r}\right)^{n-1} dr\right] \tag{27}$$

Using $|\tau_H| = \tau_H$ and using equations (23) and (26) in equation (15) and then integrating from r to R(z), the initial approximation to the velocity u_H^{***} in the region $\lambda_2 \le r \le R(z)$ is given by

$$u_H^{***} = P^n\left[\int_r^{R(z)} \left(\frac{r^2 - \lambda^2}{r}\right)^n dr - n\beta\int_r^{R(z)} \left(\frac{r^2 - \lambda^2}{r}\right)^{n-1} dr\right] \tag{28}$$

By the continuity of the velocity distribution throughout the flow field, we have the condition that

$$u_H^*|_{r=\lambda_1} = u_p = u_H^{***}|_{r=\lambda_2} \tag{29}$$

where u_H^* and u_H^{***} are fluid velocity distribution in the region $K \le r \le \lambda_1$ and $\lambda_2 \le r \le R(z)$ respectively

$$\Rightarrow P^n \left[\begin{array}{l} \int_K^{\lambda_1} \left(\frac{\lambda^2 - r^2}{r} \right)^n dr - n\beta \int_K^{\lambda_1} \left(\frac{\lambda^2 - r^2}{r} \right)^{n-1} dr \\ - \int_{\lambda_2}^{R(z)} \left(\frac{r^2 - \lambda^2}{r} \right)^n dr + n\beta \int_{\lambda_2}^{R(z)} \left(\frac{r^2 - \lambda^2}{r} \right)^{n-1} dr \end{array} \right] = 0 \qquad (30)$$

By substituting the value of λ^2 and λ_2 in the equation (30), we get

$$P^n \left[\begin{array}{l} \int_K^{\lambda_1} \left(\frac{\lambda_1(\lambda_1+\beta) - r^2}{r} \right)^n dr - n\beta \int_K^{\lambda_1} \left(\frac{\lambda_1(\lambda_1+\beta) - r^2}{r} \right)^{n-1} dr \\ - \int_{\lambda_2}^{R(z)} \left(\frac{r^2 - \lambda_1(\lambda_1+\beta)}{r} \right)^n dr + n\beta \int_{\lambda_2}^{R(z)} \left(\frac{r^2 - \lambda_1(\lambda_1+\beta)}{r} \right)^{n-1} dr \end{array} \right] = 0 \qquad (31)$$

The integrals are evaluated as

$$\int \left(\frac{\lambda^2 - r^2}{r} \right)^n dr = \left(\frac{r^{1-n}\lambda^{2n}}{1-n} - n\frac{r^{3-n}\lambda^{2n-2}}{3-n} \right)$$

$$\int \left(\frac{\lambda^2 - r^2}{r} \right)^{n-1} dr = \left(\frac{r^{2-n}\lambda^{2(n-1)}}{2-n} - (n-1)\frac{r^{4-n}\lambda^{2n-4}}{4-n} \right) \qquad \int \left(\frac{r^2 - \lambda^2}{r} \right)^n dr = \left(\frac{r^{n+1}}{n+1} + n\frac{\lambda^2 r^{n-1}}{1-n} \right)$$

$$\int \left(\frac{r^2 - \lambda^2}{r} \right)^{n-1} dr = \left(\frac{r^n}{n} + (n-1)\frac{\lambda^2 r^{n-2}}{2-n} \right)$$

By substituting value of the integrals, we get

$$P^n \left[\begin{array}{l} \left(\frac{{\lambda_1}^{1-n}(\lambda_1(\lambda_1+\beta))^n}{1-n} - n\frac{{\lambda_1}^{3-n}\lambda^{2n-2}}{3-n} \right) \\ - \left(\frac{K^{1-n}(\lambda_1(\lambda_1+\beta))^n}{1-n} - n\frac{K^{3-n}\lambda^{2n-2}}{3-n} \right) \\ -n\beta \left[\left(\frac{{\lambda_1}^{2-n}(\lambda_1(\lambda_1+\beta))^{n-1}}{2-n} - (n-1)\frac{{\lambda_1}^{4-n}(\lambda_1(\lambda_1+\beta))^{n-2}}{4-n} \right) - \right. \\ \left. \left(\frac{K^{2-n}(\lambda_1(\lambda_1+\beta))^{n-1}}{2-n} - (n-1)\frac{K^{4-n}(\lambda_1(\lambda_1+\beta))^{n-2}}{4-n} \right) \right] \\ - \left[\left(\frac{(R(z))^{n+1}}{n+1} + n\frac{(\lambda_1(\lambda_1+\beta))(R(z))^{n-1}}{1-n} \right) - \left(\frac{{\lambda_2}^{n+1}}{n+1} + n\frac{(\lambda_1(\lambda_1+\beta)){\lambda_2}^{n-1}}{1-n} \right) \right] + n\beta \\ \left[\left(\frac{(R(z))^n}{n} + (n-1)\frac{(\lambda_1(\lambda_1+\beta))(R(z))^{n-2}}{2-n} \right) - \left(\frac{{\lambda_2}^n}{n} + (n-1)\frac{(\lambda_1(\lambda_1+\beta)){\lambda_2}^{n-2}}{2-n} \right) \right] \end{array} \right] = 0$$

From the above newly proposed equations the plug flow region boundary value for λ_1 can be found using the Regula-falsi method and the using the relation in equation (23) the value λ_2 can be found. The single Herschel-Bulkley fluid model steady flow rate is given by

$$Q = 8\int_{KR}^{R(z)} urdr = 8\left[\int_K^{\lambda_1} {u_H}^* rdr + \int_{\lambda_1}^{\lambda_2} u_p rdr + \int_{\lambda_2}^{R(z)} {u_H}^{***} rdr \right]$$

$$Q = 8\left[Q_1 + Q_2 + Q_3 \right]$$

$$Q_1 = \int_{x=K}^{\lambda_1} P^n \begin{bmatrix} \left(\frac{\lambda_1^2 - x^2}{2}\right)\left(\frac{\lambda^2 - x^2}{x}\right)^n dx \\ -n\beta\left(\frac{\lambda_1^2 - x^2}{2}\right)\left(\frac{\lambda^2 - x^2}{x}\right)^{n-1} dx \end{bmatrix}$$

$$Q_2 = \int_{x=K}^{\lambda_1} P^n \begin{bmatrix} \left(\frac{\lambda_2^2 - \lambda_1^2}{2}\right)\left(\frac{\lambda^2 - x^2}{x}\right)^n dx \\ -n\beta\left(\frac{\lambda_2^2 - \lambda_1^2}{2}\right)\left(\frac{\lambda^2 - x^2}{x}\right)^{n-1} dx \end{bmatrix}$$

$$Q_3 = P^n \begin{bmatrix} \int_{x=\lambda_2}^{R(z)} \left(\frac{x^2 - \lambda_2^2}{2}\right)\left(\frac{x^2 - \lambda^2}{x}\right)^n dx \\ -n\beta \int_{x=\lambda_2}^{R(z)} \left(\frac{x^2 - \lambda_2^2}{2}\right)\left(\frac{x^2 - \lambda^2}{x}\right)^{n-1} dx \end{bmatrix}$$

The steady flow rate is obtained as

$$Q = 8P^n \begin{bmatrix} -\int_{x=K}^{\lambda_1} \left(\frac{\lambda^2 - x^2}{x}\right)^n \frac{x^2}{2} dx + n\beta \int_{x=K}^{\lambda_1} \left(\frac{\lambda^2 - x^2}{x}\right)^{n-1} \frac{x^2}{2} dx \\ +\int_{x=\lambda_2}^{R(z)} \left(\frac{x^2 - \lambda^2}{x}\right)^n \frac{x^2}{2} dx - n\beta \int_{x=\lambda_2}^{R(z)} \left(\frac{x^2 - \lambda^2}{x}\right)^{n-1} \frac{x^2}{2} dx \\ +\int_{x=K}^{\lambda_1} \frac{\lambda_2^2}{2}\left(\frac{\lambda^2 - x^2}{x}\right)^n dx - n\beta \int_{x=K}^{\lambda_1} \frac{\lambda_2^2}{2}\left(\frac{\lambda^2 - x^2}{x}\right)^{n-1} dx \\ -\int_{x=\lambda_2}^{R(z)} \frac{\lambda_2^2}{2}\left(\frac{x^2 - \lambda_2^2}{2}\right) dx + n\beta \int_{x=\lambda_2}^{R(z)} \frac{\lambda_2^2}{2}\left(\frac{x^2 - \lambda^2}{x}\right)^{n-1} dx \end{bmatrix}$$

By using equation (30) in (50), we get

$$Q = 4P^n \begin{bmatrix} -\int_{x=K}^{\lambda_1} \left(\frac{\lambda^2 - x^2}{x}\right)^n x^2 dx + n\beta \int_{x=K}^{\lambda_1} \left(\frac{\lambda^2 - x^2}{x}\right)^{n-1} x^2 dx \\ +\int_{x=\lambda_2}^{R(z)} \left(\frac{x^2 - \lambda^2}{x}\right)^n x^2 dx - n\beta \int_{x=\lambda_2}^{R(z)} \left(\frac{x^2 - \lambda^2}{x}\right)^{n-1} x^2 dx \end{bmatrix}$$

The integrals are evaluated as

$$\int \left(\frac{\lambda^2 - r^2}{r}\right)^n r^2 dr = \left(\frac{r^{3-n}\lambda^{2n}}{3-n} - n\frac{r^{5-n}\lambda^{2n-2}}{5-n}\right) \qquad \int \left(\frac{\lambda^2 - r^2}{r}\right)^{n-1} r^2 dr = \left(\frac{r^{4-n}\lambda^{2(n-1)}}{4-n} - (n-1)\frac{r^{6-n}\lambda^{2n-4}}{6-n}\right)$$

$$\int \left(\frac{r^2 - \lambda^2}{r}\right)^n r^2 dr = \left(\frac{r^{n+3}}{n+3} - n\frac{\lambda^2 r^{n+1}}{n+1}\right)$$

$$\int \left(\frac{r^2 - \lambda^2}{r}\right)^{n-1} r^2 dr = \left(\frac{r^{n+2}}{n+2} - (n-1)\frac{\lambda^2 r^n}{n}\right)$$

By substituting value of the integrals, we get

$$Q = 4P^n \left[\begin{array}{l} -\left[\left(\frac{\lambda_1^{3-n}\lambda^{2n}}{3-n} - n\frac{\lambda_1^{5-n}\lambda^{2n-2}}{5-n}\right) - \left(\frac{K^{3-n}\lambda^{2n}}{3-n} - n\frac{K^{5-n}\lambda^{2n-2}}{5-n}\right)\right] \\ +n\beta\left[\left(\frac{\lambda_1^{4-n}\lambda^{2(n-1)}}{4-n} - (n-1)\frac{\lambda_1^{6-n}\lambda^{2n-4}}{6-n}\right) - \left(\frac{K^{4-n}\lambda^{2(n-1)}}{4-n} - (n-1)\frac{K^{6-n}\lambda^{2n-4}}{6-n}\right)\right] \\ +\left[\left(\frac{(R(z))^{n+3}}{n+3} - n\frac{\lambda^2(R(z))^{n+1}}{n+1}\right) - \left(\frac{\lambda_2^{n+3}}{n+3} - n\frac{\lambda^2\lambda_2^{n+1}}{n+1}\right)\right] \\ -n\beta\left[\left(\frac{(R(z))^{n+2}}{n+2} - (n-1)\frac{\lambda^2(R(z))^n}{n}\right) - \left(\frac{\lambda_2^{n+2}}{n+2} - (n-1)\frac{\lambda^2\lambda_2^n}{n}\right)\right] \end{array} \right]$$

The wall shear stress in the artery can be obtained by

$$\tau_w = \left[\frac{P}{r}\left(\mathrm{r}^2 - \lambda^2\right)\right]_{r=R(z)}$$

The frictional resistance per unit length of the artery is given by

$$\Lambda = \frac{P}{Q}$$

RESULTS AND DISCUSSIONS

The aim of the present study is to discuss the effects of characteristics of steady flow of blood through a catheterized tapered artery. In particular, the effects of catheterization, non-Newtonian nature of the blood, plug flow velocity, flow rate, wall shear stress and frictional resistance have been discussed. Though the range of the yield stress τ_y for blood of normal subject is 0.01–0.06 dyn/s^2, the non-Newtonian effects are more pronounced when the value of the yield stress increases. The range 0.0 – 0.25 is used to pronounce the effects of the non-dimensional yield stress τ_y, since this range is more suitable for all vessels through which a catheter is inserted. The value of the catheter radius ratio K has been taken in the range 0.1–0.3 to accommodate all the types of catheters. The steady pressure gradient *P* value is usually taken as 1.0. Here it is taken as P = 1.0 – 3.0. The value of the angle of tapering α has been taken in the range 0.01 – 0.05.

Yield Plane Locations

The effect of finite yield stress is that the fluid exhibits solid-like behavior or plug flow in regions where the shear stress is less than the yield stress. The location of a point where the shear stress is equal to the yield stress is called a yield point and the locus of such points is called yield surface or yield plane. In the case of a tube flow, there is only one yield plane, whereas for annular flow there are two yield planes $r = \lambda_1$ and $r = \lambda_2$ and these two yield planes form the boundary of the plug flow region. It is noted that $\beta(= \lambda_2 - \lambda_1)$ is the width of the plug plug flow region. For steady flow, the yield plane locations do not change during the course of motion, but they change with respect to the other parameters.

Table 1. Yield plane values for the single fluid model for the various pressure gradients

Yield stress τ_y	Yield plane values for Single fluid HB					
	For P=1 λ_1	For P=1 λ_2	For P=2 λ_1	For P=2 λ_2	For P=3 λ_1	For P=3 λ_2
0.1	0.55	0.65	0.56	0.61	0.585	0.618333
0.15	0.53	0.68	0.55	0.625	0.575	0.625
0.2	0.5	0.7	0.54	0.64	0.565	0.631667

P-Pressure gradient, τ_y - yield stress, λ_1, λ_2 – Boundary layers of Plug flow regions.

The width of the plug flow region increases with the increase of the yield stress, and the reverse behavior is noticed when the steady state pressure gradient increases when all the other parameters are kept fixed.

Plug Flow Velocity

Table 2. Plug flow velocity u_p for the various pressure gradient P and catheter radius ratio K

Yield stress τ_y	Single fluid HB model Plug flow velocity (u_p)					
	P=1,K=0.1	P=1,K=0.3	P=2,K=0.1	P=2,K=0.3	P=3,K=0.1	P=3,K=0.3
0.1	0.41488	0.09159	0.81506	0.20003	1.31435	0.33771
0.15	0.39890	0.08091	0.84210	0.19634	1.29395	0.32715
0.2	0.39788	0.07722	0.80971	0.19510	1.21565	0.29343

It is found that the plug flow velocity decreases slowly with the increase of the yield stress. It is also noted that the plug flow velocity decreases significantly with the increase of the catheter radius ratio K when all the other parameters kept constant.

Wall Shear Stress

The variation of wall shear stress with the catheter radius ratio for the single fluid model and yield stress with P = 1, 2 and 3 has been calculated. It is found that the plug flow velocity increases with the increase of the yield stress. It is also noted that the plug flow velocity increases significantly with the increase of the catheter radius ratio K when all the other parameters kept constant.

Table 3. Wall shear stress τ_w for the single fluid model for various Pressure gradients P and Yield stress τ_y

Yield stress τ_y	HB Single fluid Wall shear stress τ_w		
	For P=1,K=0.1	For P=2,K=0.2	For P=3,K=0.3
0.1	0.269303	0.578077	0.802608
0.15	0.27317	0.583011	0.812008
0.2	0.283171	0.588745	0.821942

Flow Rate

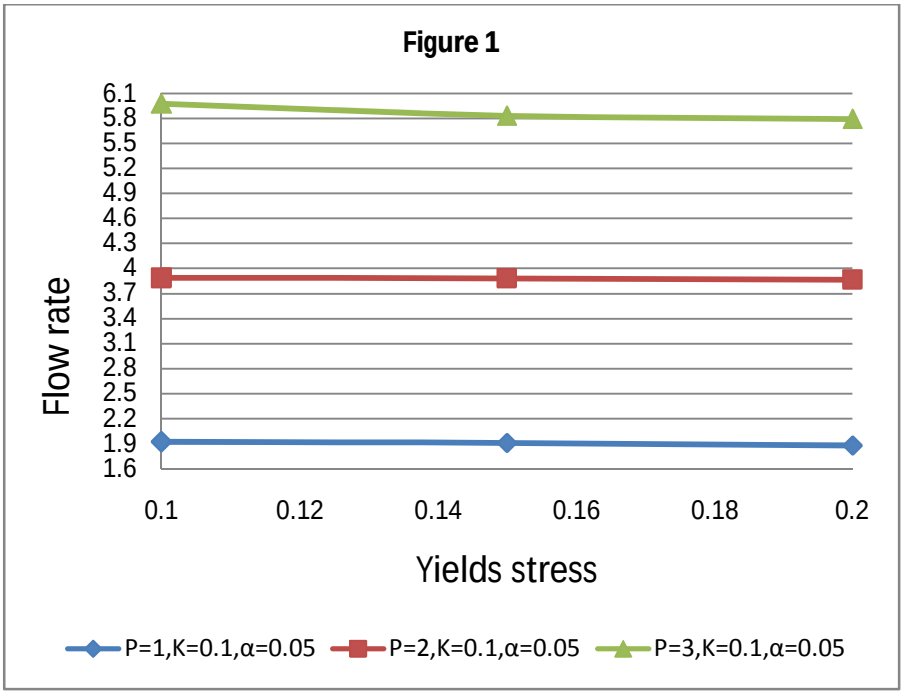

Figure 1: Flow rate for the variation of pressure gradient for different Yield stress with n=0.95

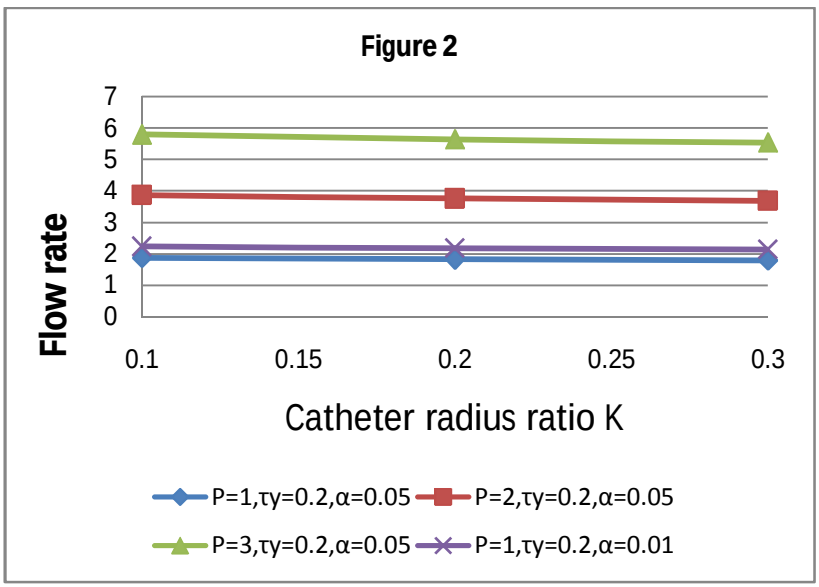

Figure 2: Flow rate for the variation of angle of tapering with pressure gradient for different Catheter radius ratio K with n=0.95

Figure 1 and 2 shows the variation of flow rate with catheter radius ratio for different values of angle of tapering α and pressure gradient P with n= 0.95, τ_y =0.2 at axial distance z = 0. It is clear that the flow rate decreases slowly with the increase of the catheter radius ratio K. Furthermore the increasing values of the angle of tapering α , the flow rate decreases. There is increase in the values of the flow rate with the increase of the pressure gradient when the other parameters are kept constant.

Frictional Resistance

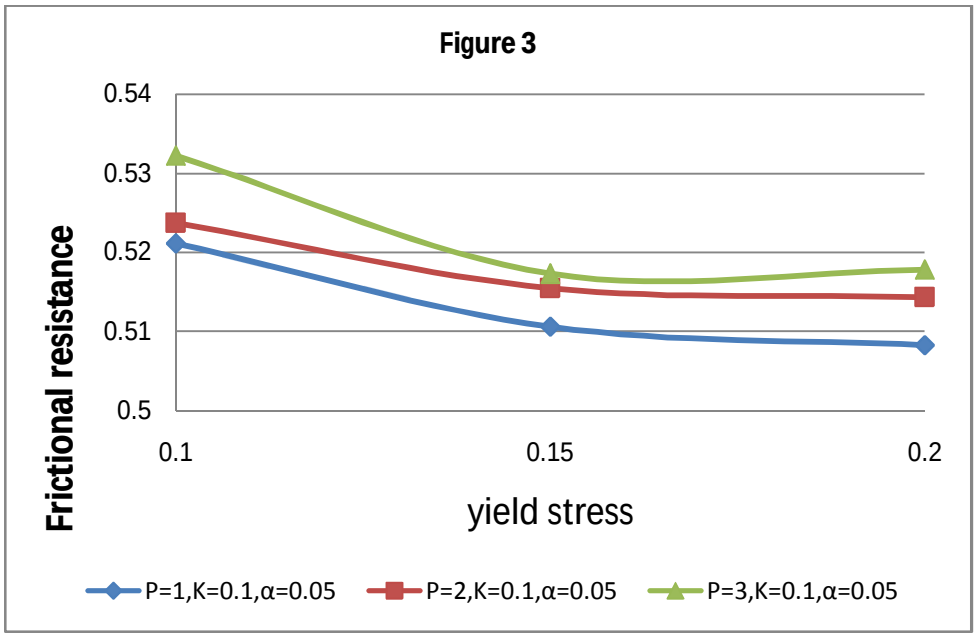

Figure 3: Frictional resistance for the variation of pressure gradient for different Yield stress with n=0.95

Figure 3 shows the variation of frictional resistance with yield stress for different values of pressure gradient P with n= 0.95, K=0.1 at axial distance z = 0. There is decrease in the values of the frictional resistance with the increase of the pressure gradient when the other parameters are kept constant.

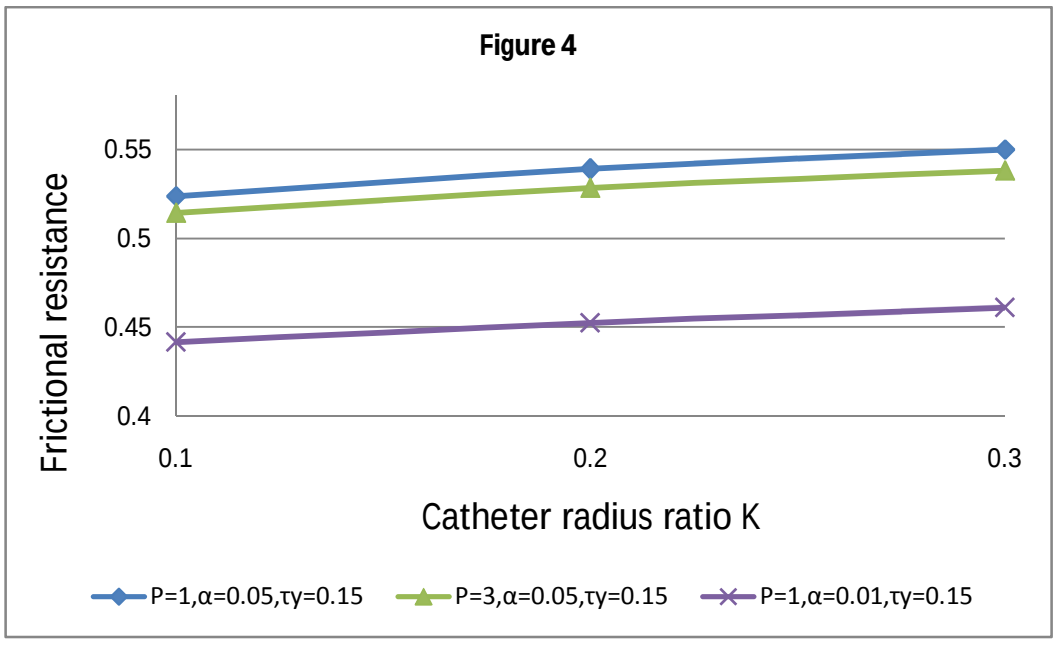

Figure 4: Frictional resistance for the variation of angle of tapering with pressure gradient for different Catheter radius ratio K with n=0.95

Figure 4 shows the variation of frictional resistance with catheter radius ratio K for different values of angle of tapering α and pressure gradient P with n= 0.95, τ_y =0.15 at axial distance z = 0. It is clear that the frictional resistance increases with the increase of the catheter radius ratio K. Furthermore the increasing values of the angle of tapering α , the frictional resistance increases. There is decrease in the values of the frictional resistance with the increase of the pressure gradient when the other parameters are kept constant.

Conclusion and Future study

The blood flow through a catheterized tapered artery has been mathematically modeled. The width of the plug flow region increases with the increase of the yield stress, and the reverse behavior is noticed when the steady state pressure gradient increases when all the other parameters are kept fixed. It is observed that the plug flow velocity and flow rate decrease while the wall shear stress and resistance to flow increase when the yield stress or catheter radius ratio or angle of tapering increases while all the other parameters held fixed. By using the present model, physicians can be more accurate in predicting the post- catheterization flow quantities so that they can plan and analyze a suitable treatment before entering the operation. Hence, in view of the above discussion, it is concluded that the present analysis is believed to yield some good improvement in the studies of blood flow through catheterized arteries. An extension of this study to the pulsatile flow would be more interesting and may explain the more realistic situation of the blood flow. Further, the inclusion of the elastic nature of the blood vessels in the study will have more applicability to the medical field.

REFERENCES

Anderson, H.V., Roubin, G.S., Limgruber, P.P., Cox, W.R., Douglas, J.S. Jr, King. S.B. and Gruentzig, A.R. 1986. Measurement of Transtenotic Pressure Gradient during Perculateous Transluminal Coronary Angioplasty Circulation 73: 1223-1230.

D.S. Sankar, K. Hemalatha. 2006. Pulsatile flowof Herschel–Bulkley fluid through stenosed Arteries - A mathematical model, International Journal of Non-Linear Mechanics. 41:979 – 990.

D.S. Sankar, Usik Lee. 2011. Nonlinear mathematical analysis for blood flow in a constricted artery under periodic body acceleration. Commun Nonlinear Sci Numer Simulat. 16, 4390–4402.

D.S.Sankar , K. Hemalatha. 2007. Pulsatile flow of Herschel–Bulkley fluid through catheterized arteries – A mathematical model. Applied Mathematical Modelling. 31:1497–1517.

D.S.Sankar and Ahmad Izani Md. Ismail. 2009, Two-Fluid Mathematical Models for Blood Flow in Stenosed Arteries: A Comparative Study. Hindawi Publishing Corporation Boundary Value Problems. 10, 1155.

Demiray H.2003. Weakly non-linears waves in a fluid with variable viscosity contained in a presented than elastic tube, Chaos Soliton Fract 36:196-202.

Dhar P, Seshadri V, Jayaraman G, 1995. Hemorheological Changes in the Patients of Myocardial Infarction and Stroke, Clinical Hemorheology and Micro circulation, STM Publishing House, 15(5): 715-727.

Kapur J.N, Bhat B.S, Sacheti N.C,1992. Non- Newtonian Fluid Flows (A Survey Monograph), Pragati Prakashan, Meerut, India.

Mac Mahon T. A, Clark C, Murthy V. S, and Shapiro A. H, 1971. Intra-aortic balloon experiment in a lumped-element hydraulic model of the circulation, Journal of Biomechanics, Elsevier, 4: 335–350.

Merrill E.W,1965. Rheology of Human Blood and Some Speculations on its Role in Vascular Homeostasis Biomechanical Mechanisms in Vascular Homeostasis and and Intravascular Thrombosis, P.N. Sawyer (ed.), Appleton Century Crofts, New York, 127-137.

Nerem R.M,1992.Vascular fluid mechanics, the arterial wall, and atherosclerosis. Journal of Biomechanical Engineering , ASME, 114, 274-282.

Oka, S.1973.Pressure Development in a Non- Newtonian Flow Through a Tapered Tube. Biorheology. 10: 207-212.

Pralhad R.N, and Schultz D.H,2004. Modeling of arterial stenosis and its applications to blood diseases, Mathematical Biosciences, Elsevier, 190, 203-220.

Prashanta Kumar Mandal, Santabrata Chakravarty, Arabinda Mandal, Norsarahaida Amin. 2007. Effect of body acceleration on unsteady pulsatile flow of non-newtonian fluid through a stenosed artery, Applied Mathematics and Computation, 189,766–779.

Prashanta Kumar Mandal. 2005. An unsteady analysis of non-Newtonian blood flow through tapered arteries with a stenosis. International Journal of Non-Linear Mechanics. 40, 151 – 164.

R. K. Dash, G. Jayaraman, and K. N. Metha. 1999. Flow in a catheterized curved artery with stenosis," Journal of Biomechanics, 32:. 49–61.

R. Ponalagusamy, R. Tamil Selvi. , 2011. A study on two-layered model (Casson-newtonian) for Blood flow through an arterial stenosis: Axially variable slip velocity at the wall. 00162-1 : PII: S0016- 0032.

R. Wilson, M. R. Johnson, M. L, Marcus, et al., 1988. The effect of coronary angioplasty on coronary flow reserve, Circulation, Journal of the American Heart Association, 77: 873–885.

Rao A.R, Padmavathi K, 1997. Mathematical models for catheter movement in blood vessels, Journal of Mathematics and Mathematical Biosciences, Gwalior Academy of Mathematical Sciences, 1(1): 57-78.

Shukla J. B, Parihar R. S, and Gupta S. P, 1980. Effects of peripheral layer viscosity on blood flow thorough the artery with mild stenosis, Bulletin of Mathematical Biorheology, Springer, 42(6): 797-805.

Srivastava, L.M. and Srivastava, V.P.1983. On Two-Phase Model of Pulsatile Blood Flow with Entrance Effects. Biorheol.,20: 761-777.

Srivastava, V. P. 1995, Arterial blood flow through a nonsymmetrical stenosis with applications. Jpn. J. Appl. Phys., 34, 6539-6545.

Srivastava, V. P. A theoretical model for blood flow in small vessels. Applications and Applied Mathematics, v 2, pp. 51-65, 2007.

Srivastava, V.P.1996. Two-phase Model of Blood Flow Through Stenosed Tubes in the Presence of a Peripheral Layer. J. Biomech., 29, 1377-1382.

Wilson R.F, Johnson M.R, Marcus M.L, Aylward P.E.G, Skorton D.J, Collings S, and White C.W,1985. The effect of coronary angioplasty on coronary flow reserve, Circulation, Journal of the American Heart Association, 77: 873- 885.

****